Published for SISSA by Springer

Received: January 12, 2015
Revised: February 13, 2015
Accepted: April 7, 2015
Published: May 5, 2015

Determination of the branching fractions of $B^0_s \to D^\mp_s K^\mp$ and $B^0 \to D^-_s K^+$

The LHCb collaboration

E-mail: l.bel@cern.ch

Abstract: Measurements are presented of the branching fractions of the decays $B^0_s \to D^\mp_s K^\mp$ and $B^0 \to D^-_s K^+$ relative to the decays $B^0_s \to D^-_s \pi^+$ and $B^0 \to D^- \pi^+$, respectively. The data used correspond to an integrated luminosity of $3.0\,\text{fb}^{-1}$ of proton-proton collisions. The ratios of branching fractions are

$$\frac{\mathcal{B}(B^0_s \to D^\mp_s K^\mp)}{\mathcal{B}(B^0_s \to D^-_s \pi^+)} = 0.0752 \pm 0.0015 \pm 0.0019$$

and

$$\frac{\mathcal{B}(B^0 \to D^-_s K^+)}{\mathcal{B}(B^0 \to D^- \pi^+)} = 0.0129 \pm 0.0005 \pm 0.0008,$$

where the uncertainties are statistical and systematic, respectively.

Keywords: Hadron-Hadron Scattering, Branching fraction, B physics, Flavor physics

ArXiv ePrint: 1412.7654

doi:10.1007/JHEP05(2015)019

JHEP05(2015)019

Contents

1 Introduction

This paper presents the measurements of the branching fractions of the decays $B^0_s \to D^\mp_s K^\pm$ and $B^0 \to D^-_s K^+$, relative to those of the decays $B^0_s \to D^-_s \pi^+$ and $B^0 \to D^- \pi^+$, respectively. The $B^0_s \to D^\mp_s K^\pm$ system is of interest as it offers a prime opportunity to measure *CP* violation in the interference between mixing and decay [1, 2]. The B^0_s meson can decay into both charge-conjugate decays, providing sensitivity to the CKM angle γ [3]. The decays $B^0_s \to D^\mp_s K^\pm$ and $B^0_s \to D^-_s \pi^+$ occur predominantly through colour-allowed tree diagrams (see figure 1). A lower bound on the ratio of the $B^0_s \to D^\mp_s K^\pm$ and $B^0_s \to D^-_s \pi^+$ branching fractions was derived, $\mathcal{B}(B^0_s \to D^\mp_s K^\pm)/\mathcal{B}(B^0_s \to D^-_s \pi^+) \geq 0.080 \pm 0.007$ [4], with minimal external experimental and theoretical input. Using SU(3) flavour symmetry, and measurements of $B^0 \to D^- \pi^+$ decays at the B-factories, a prediction for the ratio of branching fractions was calculated, $\mathcal{B}(B^0_s \to D^\mp_s K^\pm)/\mathcal{B}(B^0_s \to D^-_s \pi^+) = 0.086^{+0.009}_{-0.007}$ [4], where the uncertainty includes contributions from non-factorisable effects [5] and from possible SU(3)-breaking effects of up to 20%.

The CDF and Belle collaborations have pioneered the study of this ratio [6, 7], followed by the LHCb collaboration, which measured a ratio about 1.8 standard deviations below the theoretical bound [8], using data corresponding to an integrated luminosity of 336 pb^{-1}.

The decay $B^0 \to D^-_s K^+$ proceeds through the colour-suppressed W-exchange diagram and the branching fraction determination allows the size of the W-exchange amplitude to be estimated, for example in the $B^0_s \to D^\mp_s K^\pm$ decay, as used e.g. in ref. [4]. The existing branching fraction measurements by BaBar and Belle, $\mathcal{B}(B^0 \to D^-_s K^+) = (2.9 \pm 0.4\,(\text{stat}) \pm 0.2\,(\text{syst})) \times 10^{-5}$ [9] and $(1.91 \pm 0.24\,(\text{stat}) \pm 0.17\,(\text{syst})) \times 10^{-5}$ [10], respectively, show a difference of about 1.8 standard deviations, and suggest that an enhancement of the branching fraction due to rescattering effects is small [11]. Note that throughout this paper, charge conjugation is implied, and thus that the branching fraction $\mathcal{B}(B^0_{(s)})$ corresponds to the average of the branching fraction of the $B^0_{(s)}$ decay and the $\overline{B}{}^0_{(s)}$ decay.

JHEP05(2015)019

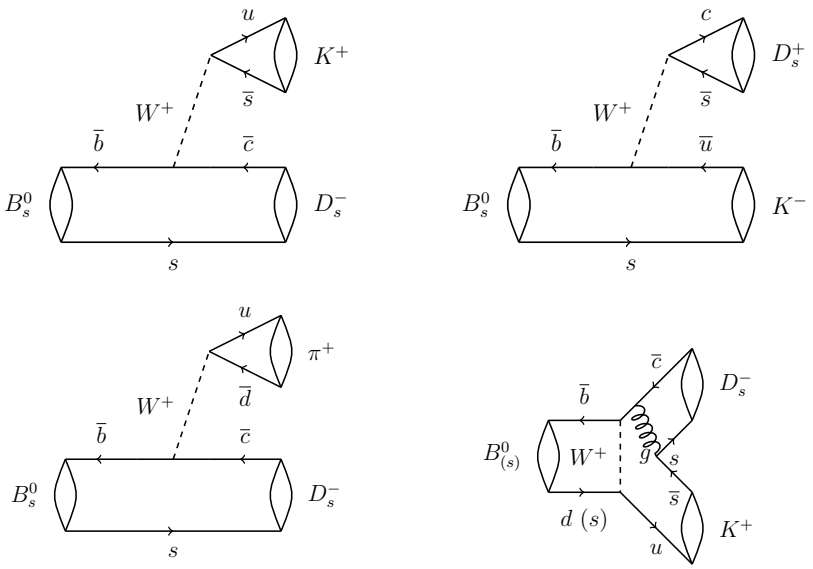

Figure 1. Feynman diagrams of the processes under study. The upper diagrams represent the two tree topologies in which a B_s^0 meson decays into the $D_s^{\mp}K^{\pm}$ final state, and the lower diagrams show the tree diagram of $B_s^0 \to D_s^- \pi^+$ and the W-exchange topology of $B_{(s)}^0 \to D_s^- K^+$.

The pp-collision data used in this analysis correspond to an integrated luminosity of $3.0\,\text{fb}^{-1}$, of which $1.0\,\text{fb}^{-1}$ was collected by LHCb in 2011 at a centre-of-mass energy of $\sqrt{s} = 7\,\text{TeV}$, and the remaining $2.0\,\text{fb}^{-1}$ in 2012 at $\sqrt{s} = 8\,\text{TeV}$.

The LHCb detector [12] is a single-arm forward spectrometer covering the pseudorapidity range $2 < \eta < 5$, designed for the study of particles containing b or c quarks. The detector includes a high-precision tracking system consisting of a silicon-strip vertex detector surrounding the pp interaction region, a large-area silicon-strip detector located upstream of a dipole magnet with a bending power of about 4 Tm, and three stations of silicon-strip detectors and straw drift tubes placed downstream of the magnet. The polarity of the magnet is reversed periodically throughout data-taking. The tracking system provides a measurement of momentum, p, with a relative uncertainty that varies from 0.4% at low momentum to 0.6% at 100 GeV/c. The minimum distance of a track to a primary vertex, the impact parameter, is measured with a resolution of $(15 + 29/p_{\text{T}})\,\mu\text{m}$, where p_{T} is the component of p transverse to the beam, in GeV/c. Different types of charged hadrons are distinguished using information from two ring-imaging detectors.

The trigger consists of a hardware stage, based on information from the calorimeter and muon systems, followed by a software stage, which applies a full event reconstruction. The software trigger requires a two-, three- or four-track secondary vertex with a significant displacement from the primary pp interaction vertices (PVs). At least one charged particle must have a transverse momentum $p_{\text{T}} > 1.7\,\text{GeV}/c$ and be inconsistent with originating from the PV. A multivariate algorithm [13] is used for the identification of secondary vertices consistent with the decay of a b hadron.

In the simulation, pp collisions are generated using Pythia [14, 15] with a specific

JHEP05(2015)019

Selection efficiency (%)	Kinematic	PID	Total
$B^0 \to D^- \pi^+$	1.89 ± 0.01	74.29 ± 0.07	1.40 ± 0.01
$B^0_s \to D^-_s \pi^+$	1.92 ± 0.02	67.10 ± 0.09	1.29 ± 0.01
$B^0_s \to D^\mp_s K^\pm$	2.08 ± 0.01	55.52 ± 0.17	1.15 ± 0.01
$B^0 \to D^-_s K^+$	1.70 ± 0.03	58.11 ± 0.82	0.99 ± 0.02

Table 1. Kinematic and PID selection efficiencies for each signal decay, as determined from simulated events and data, respectively. "PID" refers to the selection efficiencies of the PID requirements only, while "Kinematic" refers to the remaining event selection. The kinematic efficiencies represent weighted averages determined from events simulated at $\sqrt{s} = 7\,\text{TeV}$ (34%) and $\sqrt{s} = 8\,\text{TeV}$ (66%). The binomial uncertainties result from the size of the simulated samples.

LHCb configuration [16]. Decays of hadronic particles are described by EvtGen [17]. The interaction of the generated particles with the detector and its response are implemented using the Geant4 toolkit [18, 19] as described in ref. [20].

2 Event selection

Candidate $B^0_{(s)}$ mesons are reconstructed by combining a $D^\pm_{(s)}$ candidate decaying into three light hadrons, $D^- \to K^+\pi^-\pi^-$ or $D^-_s \to K^+K^-\pi^-$, with an additional pion or kaon (the "bachelor" particle). Each of the four final-state light hadrons is required to have a good track quality, high momentum and transverse momentum, and a large impact parameter with respect to the primary vertex. The contribution from charmless $B^0_{(s)}$ decays, such as $B^0_s \to K^+K^-\pi^+\pi^-$, is suppressed by requiring the $D^\pm_{(s)}$ candidate to have a significant flight distance from the reconstructed $B^0_{(s)}$ decay vertex, and by requiring its mass to fall within a small mass window of $^{+22}_{-24}\,\text{MeV}/c^2$ around the $D^\pm_{(s)}$ mass [21]. To reduce the combinatorial background, a multivariate algorithm is applied. This boosted decision tree (BDT) [22, 23] is identical to that used in the analysis of the *CP* asymmetry in $B^0_s \to D^\mp_s K^\pm$ decays [3], and was trained with $B^0_s \to D^-_s \pi^+$ candidates from data, using a weighted data sample based on the *sPlot* technique [24] as signal and candidates with an invariant mass greater than $5445\,\text{MeV}/c^2$ as background. The variables with the highest discriminating power are found to be the difference between the χ^2 from the vertex fit of the associated PV reconstructed with and without the considered b-hadron candidate, the p_T of the final-state particles, and the angle between the b-hadron momentum vector and the vector connecting its production and decay vertices.

Misidentification of particles leads to peaking backgrounds in the signal region, for example $B^0_s \to D^-_s \pi^+$ events reconstructed as $B^0_s \to D^\mp_s K^\pm$ candidates. Pions and kaons in these decays are required to satisfy particle identification (PID) requirements, and approximately 60% of the signal is retained while over 99% of the background is rejected. The efficiencies of these requirements are determined by studying kinematically selected $D^{*+} \to D^0(\to K^-\pi^+)\pi^+$ and $\Lambda \to p\pi^-$ decays obtained from data, which provide high-purity PID.

In the $B^0 \to D^-\pi^+$ selection, loose PID requirements are applied since the branching fraction of the signal process is much larger than those of background decays resulting

JHEP05(2015)019

from misidentification. In the $B_s^0 \to D_s^- \pi^+$ and $B_s^0 \to D_s^\mp K^\pm$ selections, a stricter PID requirement is applied to the D_s^+ decay products, to distinguish D_s^+ and D^+ mesons. For these decays, a further selection requirement is applied to reduce the background from $\Lambda_b^0 \to \Lambda_c^+ \pi^-$ decays, where one of the D_s^+ daughters is a misidentified proton. This requirement removes any candidate which fulfils two criteria: that there is a large probability for one of the D_s^+ daughters to be a misidentified proton, and that when the D_s^+ decay is reconstructed under the Λ_c^+ hypothesis, its invariant mass falls within $21\,\mathrm{MeV}/c^2$ of the nominal Λ_c^+ mass [21]. This procedure almost fully eliminates this background. The efficiency of the selection is obtained from simulation and is summarised in table 1.

3 Signal yield determination

An unbinned maximum likelihood fit to the candidate invariant mass distribution is performed for each of the three final states, $D^-\pi^+$, $D_s^-\pi^+$, and $D_s^\mp K^\pm$. The signal shapes are parametrised by a double-sided Crystal Ball shape [25]. This function consists of a central Gaussian part, whose mean and width are free parameters, and power-law tails on both lower and upper sides, to account for energy loss due to final-state radiation and detector resolution effects. The functional form for the combinatorial background, an exponential function with an offset, is obtained from same-charge $D_s^\pm \pi^\pm$ combinations in data. All parameters of the combinatorial background are left free in the fit to data.

The physical backgrounds can be split into two categories: misidentified backgrounds, predominantly where one of the final state pions (kaons) is mistaken for a kaon (pion); and partially reconstructed backgrounds, where a neutral pion or a photon is not included in the candidate reconstruction, causing the reconstructed $B_{(s)}^0$ mass to shift to lower values. Some backgrounds fall into both categories. The number of background components considered varies per final state; the list of background components for each final state can be found in the legend of figures 2 and 3. The invariant mass shapes of these backgrounds are obtained from simulation at $\sqrt{s} = 8\,\mathrm{TeV}$, with the event selection applied. The yield of each background is a parameter in the fit, with most background components Gaussian-constrained around the expected yield normalised to the $B^0 \to D^-\pi^+$ yield obtained from data. The constraints are assigned an uncertainty of 10%, which reflects the uncertainties from production fractions, branching fractions, and reconstruction efficiencies. The resulting background yields from the fit deviate typically around one standard deviation from the expected values. The results of the fits for the three final states are shown in figures 2 and 3, and in table 2. The three fits are independent, and no parameters are shared among them.

Various consistency checks are performed for each of the fits. The fitted yield of $B_s^0 \to D_s^-\pi^+$ events reconstructed in the $D_s^\mp K^\pm$ final state, which is allowed to vary in the fit, is consistent with the expected yield based on the relative branching fraction, particle misidentification probability and reconstruction efficiency. For each of the fits, consistency is also found between the fitted yield for both magnet polarities separately and the fraction of data corresponding to that polarity. This demonstrates that the relative yields are stable as a function of time and magnet polarity.

JHEP05(2015)019

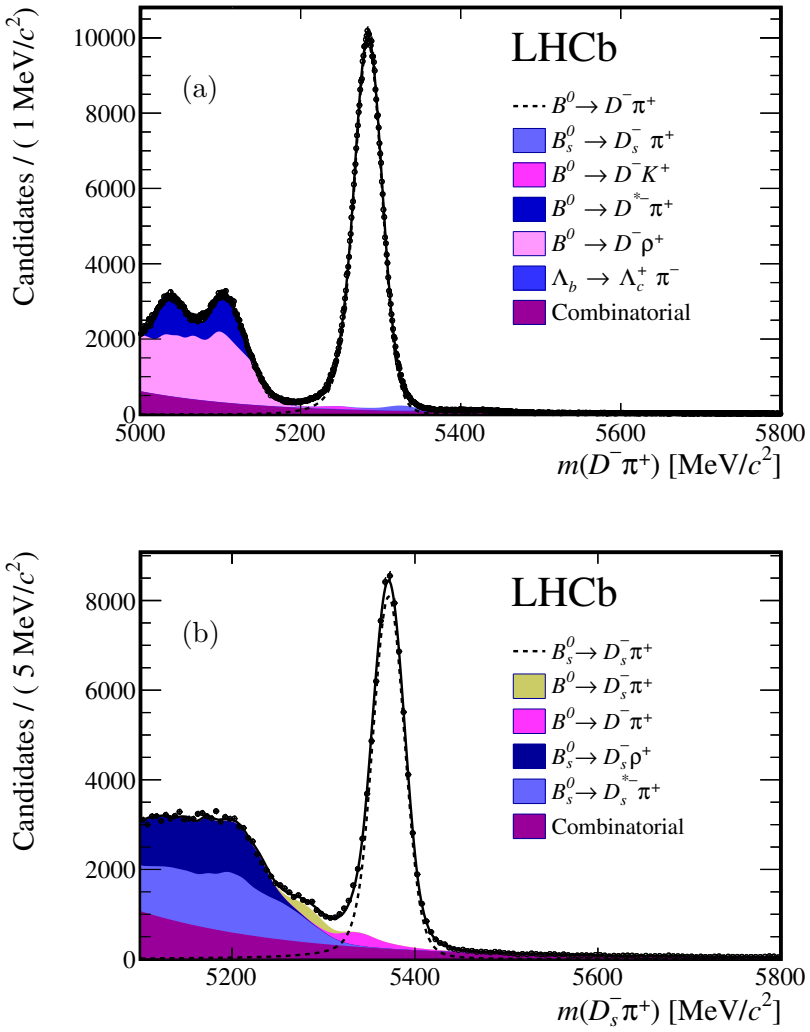

Figure 2. Results of the fits to the invariant mass distributions of the final states (a) $D^-\pi^+$ and (b) $D_s^-\pi^+$.

	Yield
$B^0 \to D^-\pi^+$	458 940 ± 959
$B_s^0 \to D_s^-\pi^+$	75 566 ± 342
$B_s^0 \to D_s^\mp K^\pm$	5 101 ± 100
$B^0 \to D_s^-K^+$	2 452 ± 98

Table 2. Yields for the four signal decay types, as obtained from the fits.

JHEP05(2015)019

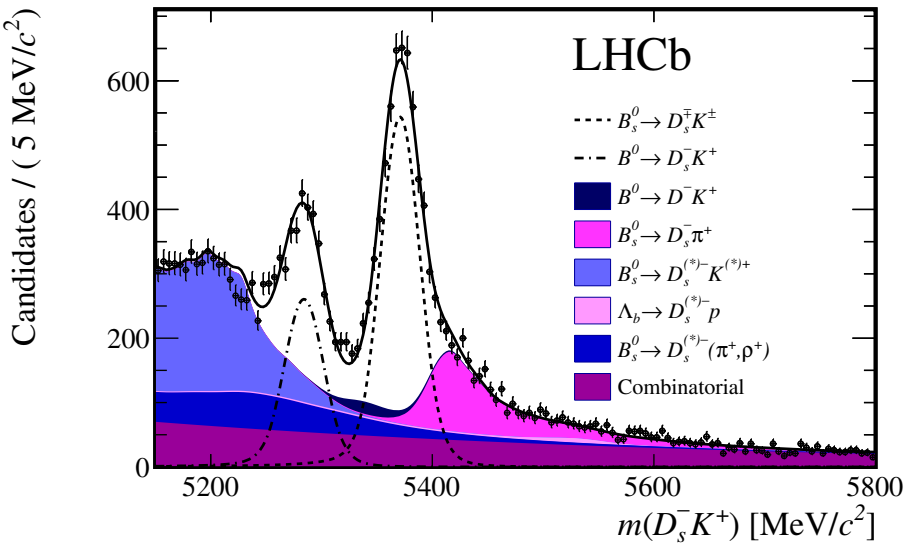

Figure 3. Result of the fit to the invariant mass distribution of the final state $D_s^{\mp} K^{\pm}$.

4 Systematic uncertainties

Systematic uncertainties arise from the fit model and the candidate selection, and are summarised in table 3. The systematic uncertainty from the fit model is determined by applying variations to the fit model and comparing the yield to the nominal result, taking the difference as a systematic uncertainty. These variations include a different combinatorial shape, fixing the signal shape tail parameters to values obtained from simulation, and using background shapes determined from simulation matching the LHCb conditions during 2011 ($\sqrt{s} = 7\,\text{TeV}$). In the $D^-\pi^+$ analysis, the fit range is reduced to start at $5100\,\text{MeV}/c^2$. In the $D_s^{\mp} K^{\pm}$ analysis, the as yet unobserved decay $\Lambda_b^0 \to D_s^- p$ is omitted from the fit.

The uncertainty on the candidate selection is separated into three parts: the uncertainty due to the kinematic selection, that due to the PID requirements on the final state pions and kaons, and that due to the hardware trigger efficiency. The first of these uncertainties is determined from the selection efficiency difference between magnet polarities in simulation, and by estimating the uncertainty on the BDT selection efficiency due to differences between data and simulation. This is calculated by reweighting simulated events to match the data more closely, and calculating the difference in BDT efficiency between those and the unweighted samples. The uncertainty on the PID efficiency and misidentification rate is estimated by comparing the PID performance measured using a simulated D^* calibration sample with that observed in simulated signal events. The systematic uncertainty from the hardware trigger efficiency arises from measured differences between the pion and kaon trigger efficiencies which are not reproduced in the simulation. The uncertainty is scaled with the fraction of events where a pion or a kaon from the reconstructed decay was responsible for triggering.

JHEP05(2015)019

Source	$\frac{B_s^0 \to D_s^{\mp} K^{\pm}}{B_s^0 \to D_s^- \pi^+}$	$\frac{B^0 \to D_s^- K^+}{B^0 \to D^- \pi^+}$
Fit model	1.1	3.6
Candidate selection	2.1	2.9
Hardware trigger	1.0	1.2
Charmless background	–	1.0
Total	2.5	4.9

Table 3. Systematic uncertainties on the ratios of branching fractions, in %, obtained as described in the text. The total uncertainty is obtained by adding the separate contributions in quadrature.

A further systematic uncertainty is added to account for possible charmless B^0 decays peaking under the $B^0 \to D_s^- K^+$ signal. Some of the uncertainties cancel in the ratios of branching fractions, leading to lower overall systematic uncertainties than those determined individually for each decay channel. The total systematic uncertainty for each ratio of branching fractions is the quadratic sum of the individual systematic uncertainties.

5 Determination of branching fractions

The ratios of branching fractions are evaluated using the expression

$$\frac{\mathcal{B}(A)}{\mathcal{B}(B)} = \frac{\varepsilon_B}{\varepsilon_A} \frac{N_A}{N_B} \frac{f_B}{f_A} \frac{\mathcal{B}_{D^{\pm}_{(s)}}}{\mathcal{B}_{D^{\pm}_{(s)}}}, \tag{5.1}$$

where ε_X, f_X and N_X are the selection efficiency, the hadronisation fraction, and the fitted yield of decay X, respectively, and $\mathcal{B}_{D^{\pm}_{(s)}}$ is the branching fraction of $D^{\pm}_{(s)}$ decays, as appropriate. The following values are used as input [21]:

$$\begin{aligned}
\mathcal{B}(B^0 \to D^- \pi^+) &= (2.68 \pm 0.13) \times 10^{-3}, \\
\mathcal{B}(B_s^0 \to D_s^- \pi^+) &= (3.04 \pm 0.23) \times 10^{-3}, \\
\mathcal{B}(D^- \to K^+ \pi^- \pi^-) &= (9.13 \pm 0.19) \times 10^{-2}, \\
\mathcal{B}(D_s^- \to K^+ K^- \pi^-) &= (5.39 \pm 0.21) \times 10^{-2}.
\end{aligned}$$

As a cross-check, a value $\mathcal{B}(B_s^0 \to D_s^- \pi^+) = (2.95 \pm 0.01\,(\text{stat})) \times 10^{-3}$ was obtained from the measured $B_s^0 \to D_s^- \pi^+$ and $B^0 \to D^- \pi^+$ yields using eq. (5.1). This measurement is compatible with the world-average value, and the central value is unchanged with respect to the previous result published by LHCb [8].

JHEP05(2015)019

The following results are obtained

$$\frac{\mathcal{B}(B_s^0 \to D_s^{\mp} K^{\pm})}{\mathcal{B}(B_s^0 \to D_s^- \pi^+)} = 0.0752 \pm 0.0015\,(\text{stat}) \pm 0.0019\,(\text{syst}),$$
$$\mathcal{B}(B_s^0 \to D_s^{\mp} K^{\pm}) = (2.29 \pm 0.05\,(\text{stat}) \pm 0.06\,(\text{syst}) \pm 0.17(\mathcal{B}_{B_s^0})) \times 10^{-4},$$
$$\frac{\mathcal{B}(B^0 \to D_s^- K^+)}{\mathcal{B}(B^0 \to D^- \pi^+)} = 0.0129 \pm 0.0005\,(\text{stat}) \pm 0.0007\,(\text{syst}) \pm 0.0004(\mathcal{B}_{D_{(s)}^{\pm}}),$$
$$\mathcal{B}(B^0 \to D_s^- K^+) = (3.45 \pm 0.14\,(\text{stat}) \pm 0.20\,(\text{syst}) \pm 0.20(\mathcal{B}_{B^0, D_{(s)}^{\pm}})) \times 10^{-5},$$

where the uncertainties labelled ($\mathcal{B}$) arise from the uncertainties on the branching fractions used as input.

The branching fractions of $B_s^0 \to D_s^{\mp} K^{\pm}$ and $B^0 \to D_s^- K^+$ presented here are more precise than the current world-average values. The result for $\mathcal{B}(B_s^0 \to D_s^{\mp} K^{\pm})/\mathcal{B}(B_s^0 \to D_s^- \pi^+)$ is compatible with theoretical expectations [4] and with the previous result from LHCb. As expected [5], the branching fraction of the decay $B^0 \to D_s^- K^+$, dominated by the W-exchange topology, is suppressed compared to the decay $B^0 \to D^- \pi^+$, which predominantly proceeds through the colour-allowed tree topology. The measured value of $\mathcal{B}(B^0 \to D_s^- K^+)$ is in good agreement with existing measurements from the BaBar collaboration [9], and is larger than the result published by the Belle collaboration [10] with a significance of more than three standard deviations.

Acknowledgments

We express our gratitude to our colleagues in the CERN accelerator departments for the excellent performance of the LHC. We thank the technical and administrative staff at the LHCb institutes. We acknowledge support from CERN and from the national agencies: CAPES, CNPq, FAPERJ and FINEP (Brazil); NSFC (China); CNRS/IN2P3 (France); BMBF, DFG, HGF and MPG (Germany); INFN (Italy); FOM and NWO (The Netherlands); MNiSW and NCN (Poland); MEN/IFA (Romania); MinES and FANO (Russia); MinECo (Spain); SNSF and SER (Switzerland); NASU (Ukraine); STFC (United Kingdom); NSF (USA). The Tier1 computing centres are supported by IN2P3 (France), KIT and BMBF (Germany), INFN (Italy), NWO and SURF (The Netherlands), PIC (Spain), GridPP (United Kingdom). We are indebted to the communities behind the multiple open source software packages on which we depend. We are also thankful for the computing resources and the access to software R&D tools provided by Yandex LLC (Russia). Individual groups or members have received support from EPLANET, Marie Skłodowska-Curie Actions and ERC (European Union), Conseil général de Haute-Savoie, Labex ENIGMASS and OCEVU, Région Auvergne (France), RFBR (Russia), XuntaGal and GENCAT (Spain), Royal Society and Royal Commission for the Exhibition of 1851 (United Kingdom).

JHEP05(2015)019

References

[1] R. Aleksan, I. Dunietz and B. Kayser, *Determining the CP-violating phase gamma*, *Z. Phys.* **C 54** (1992) 653 [INSPIRE].

[2] R. Fleischer, *New strategies to obtain insights into CP-violation through $B_s \to D_s^{\pm} K^{\mp}, D_s^{*\pm} K^{\mp}, \ldots$ and $B_d \to D^{\pm}\pi^{\mp}, D^{*\pm}\pi^{\mp}, \ldots$ decays*, *Nucl. Phys.* **B 671** (2003) 459 [hep-ph/0304027] [INSPIRE].

[3] LHCb collaboration, *Measurement of CP asymmetry in $B_s^0 \to D_s^{\mp} K^{\pm}$ decays*, *JHEP* **11** (2014) 060 [arXiv:1407.6127] [INSPIRE].

[4] K. De Bruyn et al., *Exploring $B_s \to D_s^{(*)\pm} K^{\mp}$ Decays in the Presence of a Sizable Width Difference $\Delta\Gamma_s$*, *Nucl. Phys.* **B 868** (2013) 351 [arXiv:1208.6463] [INSPIRE].

[5] R. Fleischer, N. Serra and N. Tuning, *Tests of Factorization and* SU(3) *Relations in B Decays into Heavy-Light Final States*, *Phys. Rev.* **D 83** (2011) 014017 [arXiv:1012.2784] [INSPIRE].

[6] CDF collaboration, T. Aaltonen et al., *First observation of $\bar{B}_s^0 \to D_s^{\pm} K^{\mp}$ and measurement of the ratio of branching fractions $B(\bar{B}_s^0 \to D_s^{\pm} K^{\mp})$ /$B(\bar{B}_s^0 \to D_s^{+}\pi^{-})$*, *Phys. Rev. Lett.* **103** (2009) 191802 [arXiv:0809.0080] [INSPIRE].

[7] BELLE collaboration, R. Louvot et al., *Measurement of the Decay $B_s^0 \to D_s^{-}\pi^{+}$ and Evidence for $B_s 0 \to D_s \pm K^{\pm}$ in $e^{+}e_{-}$ Annihilation at $\sqrt{s} \sim 10.87$ GeV*, *Phys. Rev. Lett.* **102** (2009) 021801 [arXiv:0809.2526] [INSPIRE].

[8] LHCb collaboration, *Measurements of the branching fractions of the decays $B_s^0 \to D_s^{\mp} K^{\pm}$ and $B_s^0 \to D_s^{-}\pi^{+}$*, *JHEP* **06** (2012) 115 [arXiv:1204.1237] [INSPIRE].

[9] BABAR collaboration, B. Aubert et al., *Measurement of the Branching Fractions of the Rare Decays $B^0 \to D_s^{(*)+}\pi^{-}$, $B^0 \to D_s^{(*)+}\rho^{-}$ and $B^0 \to D_s^{(*)-} K^{(*)+}$*, *Phys. Rev.* **D 78** (2008) 032005 [arXiv:0803.4296] [INSPIRE].

[10] BELLE collaboration, A. Das et al., *Measurements of Branching Fractions for $B^0 \to D_s^{+}\pi^{-}$ and $\bar{B}^0 \to D_s^{+} K^{-}$*, *Phys. Rev.* **D 82** (2010) 051103 [arXiv:1007.4619] [INSPIRE].

[11] M. Gronau and J.L. Rosner, *B decays dominated by $\omega^{-}\phi$ mixing*, *Phys. Lett.* **B 666** (2008) 185 [arXiv:0806.3584] [INSPIRE].

[12] LHCb collaboration, *The LHCb Detector at the LHC*, 2008 *JINST* **3** S08005 [INSPIRE].

[13] V.V. Gligorov and M. Williams, *Efficient, reliable and fast high-level triggering using a bonsai boosted decision tree*, 2013 *JINST* **8** P02013 [arXiv:1210.6861] [INSPIRE].

[14] T. Sjöstrand, S. Mrenna and P.Z. Skands, *PYTHIA 6.4 Physics and Manual*, *JHEP* **05** (2006) 026 [hep-ph/0603175] [INSPIRE].

[15] T. Sjöstrand, S. Mrenna and P.Z. Skands, *A Brief Introduction to PYTHIA 8.1*, *Comput. Phys. Commun.* **178** (2008) 852 [arXiv:0710.3820] [INSPIRE].

[16] I. Belyaev et al., *Handling of the generation of primary events in Gauss, the LHCb simulation framework*, *IEEE Nucl. Sci. Symp. Conf. Rec. (NSS/MIC)* (2010) 1155.

[17] D.J. Lange, *The EvtGen particle decay simulation package*, *Nucl. Instrum. Meth.* **A 462** (2001) 152 [INSPIRE].

[18] GEANT4 collaboration, J. Allison et al., *Geant4 developments and applications*, *IEEE Trans. Nucl. Sci.* **53** (2006) 270.

JHEP05(2015)019

[19] GEANT4 collaboration, S. Agostinelli et al., *GEANT4: A Simulation toolkit*, *Nucl. Instrum. Meth.* **A 506** (2003) 250 [INSPIRE].

[20] LHCb collaboration, *The LHCb simulation application, Gauss: Design, evolution and experience*, *J. Phys. Conf. Ser.* **331** (2011) 032023 [INSPIRE].

[21] Particle Data Group, K.A. Olive et al., *Review of particle physics*, *Chin. Phys.* **C 38** (2014) 090001.

[22] L. Breiman, J.H. Friedman, R.A. Olshen, and C.J. Stone, *Classification and regression trees*, Wadsworth international group, Belmont, California, U.S.A. (1984).

[23] R.E. Schapire and Y. Freund, *A decision-theoretic generalization of on-line learning and an application to boosting*, *J. Comp. Syst. Sci.* **55** (1997) 119.

[24] M. Pivk and F.R. Le Diberder, *SPlot: A Statistical tool to unfold data distributions*, *Nucl. Instrum. Meth.* **A 555** (2005) 356 [physics/0402083] [INSPIRE].

[25] T. Skwarnicki, *A study of the radiative cascade transitions between the Upsilon-prime and Upsilon resonances*, PhD thesis, Institute of Nuclear Physics, Krakow, 1986, [DESY-F31-86-02].

JHEP05(2015)019